Available online at www.sciencedirect.com
SCIENCE DIRECT®
Physics Letters A 316 (2003) 265–270
PHYSICS LETTERS A
www.elsevier.com/locate/pla

Combined effects of disorders and electron–electron interactions upon metal–insulator transition in 2D nonbipartite lattice

Jiaxiang Wang *, Sabre Kais

Department of Chemistry, Purdue University, West Lafayette, IN 47907, USA

Received 23 June 2003; received in revised form 6 August 2003; accepted 6 August 2003

Communicated by R. Wu

Abstract

We examined the characteristics of a metal–insulator transition on a two-dimensional nonbipartite lattice when both disorders and electron interactions are present. Using a real-space renormalization group method and finite-size scaling analysis we have found that after the disordered system transits from the insulating state to the metal one, it can reenter an insulating state if there is a further increase in the electron–electron interactions.

PACS: 71.30.+h; 89.75.Da; 71.10.Fd

Keywords: Renormalization group; Finite-size scaling; Metal–insulator transition

Ever since the discovery of the metallic properties on effectively 2D electron systems in metal-oxide–semiconductor field-effect transistor (MOSEFs) [1], there have appeared a spate of discussions and investigations over its underlying physical mechanism [2]. In experiments, as the carrier density n is increased above a critical density n_c, the conductivity σ_{dc} decreases upon lowering the temperature T (typical of an insulator) and as $n < n_c$, σ_{dc} increases upon lowering T (typical of a conductor). Because the data can be scaled onto two curves, one for the metal and the other for the insulator, this phenomenon is seen as evidence for the occurrence of a quantum-phase transition, namely the metal–insulator transition (MIT), with carrier density as the tuning parameter. But there are also other viewpoints, supported by some experiments [3,4], maintaining that there is no 2D MIT at zero temperature and the metallic behavior is attributed to the conventional, though nontrivial, electron transport. For example, two of these models are based upon electron scattering by impurities [5] and the effect of temperature dependent screening [6,7]. Thus there is, as yet, no general consensus about the origin of the metallic behavior and it remains a controversial topic.

According to the conventional one-parameter scaling theory of noninteracting electrons [8], any amount of disorders will localize the 2D electronic state and make it insulating. Moreover, the metallic state has been seen in highly mobility structures at low carrier

* Corresponding author.
E-mail address: jwang@purdue.edu (J. Wang).

0375-9601/$ – see front matter
doi:10.1016/j.physleta.2003.08.002

concentrations. Thus it is expected that the combining effect of both electron–electron interactions and the disorders are very likely to play an important role. In fact, the role of electron–electron interactions in disordered systems was recognized long ago by Finkelstein [9] and Castellanic [10], who treated the disorder in lowest order, where all interactions contributed to the leading logarithmic behavior were summed. Recently, Si and Varma [11] calculated a correction to the compressibility of a disordered system by considering the ring diagrams. Because of the perturbation nature of these methods, they cannot deal with the regime with the disorder and the interactions having comparable magnitudes. Hence most recent work has used exact diagonalization [12,13] and Monte Carlo methods [14] in the investigations. As we know, both methods suffer from intensive calculations and it is very difficult to apply them to large-size systems. To resolve this difficulty, we resort to the real-space block renormalization group (BRG) method [19]. Although this method has uncontrollable approximations, it can give us many qualitative and insightful results and show us the direction for further more accurate work. The model we use is the Anderson–Hubbard model, which is the most simple one to include the essential ingredients for our purpose, i.e., the disorder and the electron–electron interactions. We will use this model to study the charge gap and the electron localization and delocalization on a triangular half-filled lattice as shown in Fig.1. Normally there are two kinds of disorders. One is the site disorder related to the site fluctuations and the other is the bond disorder related to the hopping terms. Here we will only consider the former one. The Hamiltonian for Anderson–Hubbard model in our case can be written as,

$$H = -t \sum_{\langle i,j\rangle,\sigma} \left[c_{i\sigma}^{+} c_{j\sigma} + \text{H.c.}\right] + U \sum_{i} \left(n_{i\uparrow} - \frac{1}{2}\right)\left(n_{i\downarrow} - \frac{1}{2}\right) - \sum_{i} \varepsilon_i (n_{i\uparrow} + n_{i\downarrow}), \tag{1}$$

where t is the nearest-neighbor hopping (exchange coupling) term, U is the local repulsive interaction and μ is the chemical potential. $c_{i\sigma}^{+}$ ($c_{i\sigma}$) creates (annihilates) an electron with spin σ in the valence orbital of the dot located at site i; the corresponding number operator is $n_{i\sigma} = c_{i\sigma}^{+} c_{i\sigma}$. $\langle\cdots\rangle$ on the first sum in Eq. (1) indicates that summation is restricted to nearest-neighbor dots. H.c. denotes the Hermitian conjugate. Note that this model Hamiltonian allows only one orbital per dot. That orbital can be empty or accommodate one or two electrons. U is the repulsion of two electrons (of opposite spins) placed in the same dot. ε_i measures the fluctuation of the site energies. It is assumed that ε_i follows a Gaussian distribution with the width to be W, i.e.,

$$P(\varepsilon_i) = \frac{1}{\sqrt{2\pi W}} e^{-(\varepsilon_i - \bar{\varepsilon})^2/(2W)}, \tag{2}$$

in which the bar over ε means its average value. Initially, we use $\bar{\varepsilon} = 0$.

The essence of the BRG method is to map the above many-particle Hamiltonian on a lattice to a new one with fewer degrees of freedom and with the same low-lying energy levels [18]. Then the mapping is repeated leading to a final Hamiltonian of a seven-site hexagonal array for which we obtain an exact numerical solution.

When there is no disorder, namely $\varepsilon_i = 0$, the procedure can be summarized into three steps: first divide the N-site lattice into appropriate n_s-site blocks labeled by p ($p = 1, 2, \ldots, N/n_s$) and separate the Hamiltonian H into a intrablock part H_{B} and an interblock H_{IB},

$$H = H_{\text{B}} + H_{\text{IB}} = \sum_{p} H_p + \sum_{\langle p,p'\rangle} V_{p,p'}, \tag{3}$$

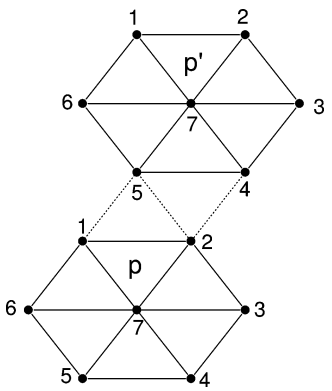

Fig. 1. Schematic diagram of the triangular lattice with hexagonal blocks. Only two neighboring blocks p and p' are drawn here. The dotted lines represent the interblock interactions and the solid lines the intrablock couplings.

where H_p is the Hamiltonian (1) for a given block and the interblock p, p' coupling is defined in Eq. (4) below.

The second step is to solve H_p exactly for the eigenvalues E_{p_i} and eigenfunctions Φ_{pi} ($i = 1, 2, \ldots, 4^{n_s}$). Then the eigenfunctions of H_{B} are constructed by direct multiplication of Φ_{pi}. The last step is to treat each block as one site on a new lattice and the correlations between blocks as hopping interactions.

The original Hilbert space has four states per site. If we are only concerned with lower lying states of the system as when studying the metal–insulator transition [17], it is not necessary to keep all the states for a block.

To make the new Hamiltonian tractable, the reduction in size should not be accompanied by a proliferation of new couplings. Then one can use an iteration procedure to solve the model. To achieve this, it is necessary to keep only 4 states in step 2. Their energies are E_i ($i = 1, 2, 3, 4$). In order to avoid proliferation of additional couplings in the new Hamiltonian, the four states kept from the block cannot be arbitrarily chosen. Some definite conditions as discussed in Ref. [15] must be satisfied. For example, the states must belong to the same irreducible representation of $C_6\nu$ symmetry group of the lattice. In particular, in order to copy the intrasite structure of the old Hamiltonian, $E_3 = E_4$ is a necessary condition. Furthermore, particle–hole symmetry of a half-filled lattice requires that $E_1 = E_2$. Further restrictions follow from the need to make extra couplings vanish. Operators in the truncated basis are denoted by a prime so that the interblock coupling of Eq. (2) is

$$V_{pp'} = \nu\lambda^2 t \sum_{\sigma} c'^{+}_{p\sigma} c'_{p'\sigma}, \tag{4}$$

where ν represents the number of couplings between neighboring blocks. The coupling strength for the border sites of a block by λ and the renormalization group equation for the coupling strength is

$$t' = \nu\lambda^2 t. \tag{5}$$

The other renormalization relation is

$$U' = 2(E_1 - E_2). \tag{6}$$

Once we introduce the disorders, because there is no exact particle–hole symmetry any more, the parameters t, U and ε_i have to be renormalized on average. In details, let us use α and β to be the block indices. Then for one block α, we can have

$$U^{\alpha} = E_1^{\alpha} + E_2^{\alpha} - 2E_3^{\alpha}, \tag{7}$$

$$\varepsilon^{\alpha} = E_2^{\alpha} - E_1^{\alpha}. \tag{8}$$

After the renormalization, the new energies ε^{α} do not obey a Gaussian distribution. In order to iterate the RG, as in Ref. [19], we adopt the following procedures:

(1) ε^{α} is forced back into a Gaussian distribution with the new width

$$W' = \overline{\left(\varepsilon^{\alpha}\right)^2} - \left(\overline{\varepsilon^{\alpha}}\right)^2. \tag{9}$$

The new Gaussian is not centered at zero since there will be a constant shift due to the electron interactions. But we can still take it to be zero by formally introducing the chemical potential.

(2) U^{α} is forced back to be constant:

$$U' = \overline{U^{\alpha}}. \tag{10}$$

(3) To get the renormalized hopping term, we will have to consider all the possible non-zero average values of the coupling between the block states. For two neighboring blocks, there are 4 possibilities:

$$t_1^{\alpha\beta} = t\left\langle \uparrow^{\alpha} 0^{\beta} \right| \sum_{\langle \alpha i, \beta j\rangle, \sigma} \left[c^{+}_{\alpha i\sigma} c_{\beta j\sigma}\right] \left| \uparrow^{\beta} 0^{\alpha} \right\rangle, \tag{11}$$

$$t_2^{\alpha\beta} = t\left\langle \uparrow \downarrow^{\alpha} 0^{\beta} \right| \sum_{\langle \alpha i, \beta j\rangle, \sigma} \left[c^{+}_{\alpha i\sigma} c_{\beta j\sigma}\right] \left| \uparrow^{\beta} \downarrow^{\alpha} \right\rangle, \tag{12}$$

$$t_3^{\alpha\beta} = t\left\langle \uparrow^{\alpha} \downarrow^{\beta} \right| \sum_{\langle \alpha i, \beta j\rangle, \sigma} \left[c^{+}_{\alpha i\sigma} c_{\beta j\sigma}\right] \left| \uparrow \downarrow^{\beta} 0^{\alpha} \right\rangle, \tag{13}$$

$$t_4^{\alpha\beta} = t\left\langle \uparrow \downarrow^{\alpha} \downarrow^{\beta} \right| \sum_{\langle \alpha i, \beta j\rangle, \sigma} \left[c^{+}_{\alpha i\sigma} c_{\beta j\sigma}\right] \left| \uparrow \downarrow^{\beta} \downarrow^{\alpha} \right\rangle. \tag{14}$$

We also force the distribution of $t^{\alpha\beta}$ into a Gaussian with mean

$$t' = \overline{t_i^{\alpha\beta}}, \tag{15}$$

and width

$$t_2' = \overline{\left(t_i^{\alpha\beta}\right)^2} - \left(\overline{t_i^{\alpha\beta}}\right)^2. \tag{16}$$

In principle, to use more blocks for averaging is always desirable. In our work, we use 7 unit blocks, which themselves form a hexagonal block.

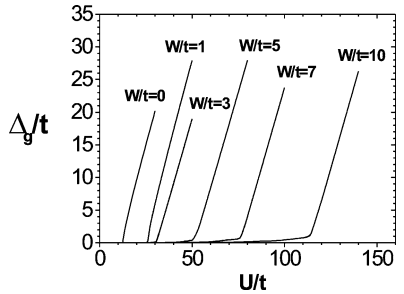

Fig. 2. Influence of the disorder (measure by W/t) over the charge gap Δ_g/t dependence upon the electron–electron interactions (U/t).

For clean systems, we have shown in our former work [15] the existence of Mott MIT at $U = 12.5$ by investigating the charge gap Δ_p, which can be expresses as the limiting value of the renormalized U,

$$\Delta_g = \lim_{n\to\infty} U'^{(n)}. \tag{17}$$

For disordered systems, as we know from the orthodox scaling theory [8], the noninteracting electrons will be localized, which leads to another kind of insulator, namely the Anderson insulator. The localization feature can be exposed by the inverse participation rate (IPR) [16] ξ defined as

$$\xi^{(4)} = \frac{N_e}{\sum_i |\langle\psi|\hat{n}_i|\psi\rangle|^4}, \tag{18}$$

where N_e is the total number of the electrons, which is equal to the site number N_s and ψ the system wave function. For totally localized electronic states in the half-filled system, half of the sites have $\langle\psi|\hat{n}_i|\psi\rangle = 2$. On the other hand, when the electron is totally delocalized, the average number of electrons per site should be $\langle\psi|\hat{n}_i|\psi\rangle = 1$. Hence the IPR $\xi^{(4)}$ will satisfy $0.125 \leqslant \xi^{(4)} \leqslant 1$ between the above two limiting cases.

In Fig. 2, we demonstrated how the disorders influence the Mott MIT. It is interesting to note that the disorder shows the effect of destablizing the Mott insulating state, namely, as we increase the disorder, part of the insulating region appears "melted" into a "metallic" state, in which the charge gap is nearly zero. At first sight, this feature quite contradicts the generally accepted viewpoints that the disorder should stabilize the insulating state. But actually they are talking about different interaction regimes with two different MIT

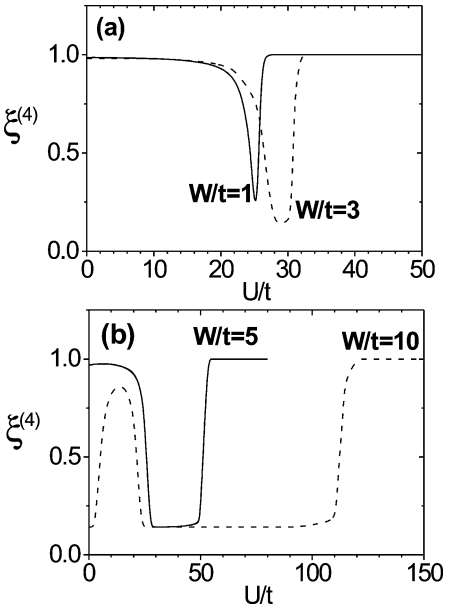

Fig. 3. Variation of the inverse participation rate (IPR, $\xi^{(4)}$) against the electron–electron interactions for different disorders with (a) $W/t = 1$ (solid line), 3 (dashed line) and (b) $W/t = 5$ (solid line), 10 (dashed line).

mechanism. Our result is obtained in a strong coupling regime with the charge gap to measure MIT (Mott MIT). As will be shown below, for weak electron–electron interactions, the disorders really stabilize the insulating state with $\xi^{(4)}$ to signature MIT (Anderson MIT).

Fig. 3 displays the evolving of electron localization and delocalization as we tune both the disorder and electron–electron interaction in the whole coupling regime. It is easy to see that all the curves follow almost the same variation patterns as we increase U for fixed disorder W. Generally speaking, there are three stages.

(1) When U is very small, the electron–electron interactions will help with the electron delocalization. This is physically understandable since the on-site repulsion will tend to rearrange the charges and make the charge-density more homogeneous. This result is consistent with the findings by Ma [19] and Caldara [20], but is different from the results from Berkovits [21] and Benenti [22]. The reason for this difference might be because Berkovits and Benenti

use spinless electrons and only consider the neighbor-site repulsion, which does not have the homogenizing effect like the on-site interaction.

(2) As we increase U further to about $U \sim W$, the electron become maximally delocalized and becomes localized again when $U > W$. The delocalization peak in the diagram is very apparent when W is, again when U for example, bigger than 10. If we interpret the shallow region around the peak to be in a metallic state, the system will then experience here a three-phase transition: insulator–metal–insulator, which is quite consistent with the experimental findings [24, 25]. Another interesting fact we might note is that, as the disorders increases, the metallic region moves further to the right of the axis, which implies that the initial insulating state becomes more stabilized. This is what we have mentioned before.

(3) After the two phase transitions, the system continues to exhibit Anderson insulating behavior until finally it evolves into a Mott insulating state with very strong electron couplings. In this regime, every site has one electron on average because of the strong on-site electron interactions.

From the above discussion, we should be able to summarize four different electronic features as U increases from zero to infinity, namely, Anderson insulator–metal–Anderson insulator–Mott insulator. This full scenario from weak to strong coupling is quite consistent with the present experiments [24,25].

One of the advantages of the BRG method is that it can be adapted easily to carry out finite-size scaling analysis of the system [23]. Thus more fundamental physics can be explored and displayed.

Fig. 4 presents our calculation results with respect to the charge gap for each fixed disorder. It is very interesting to note that as we increase the disorders, the finite-size scaling analysis provide us one critical point while W is small, which clearly represents quantum phase transition. Then the system enters some disorder/interaction range where no clear critical transition point can be identified. We call this region a "mixed" region since the two pure phases that is necessary to characterize the phase transition are difficult to define. this is demonstrated by the absence of a clear crossing point from the finite-size scaling analysis. As the disorders become stronger, two critical points are evolved out of the mixed region. From here, we can easily

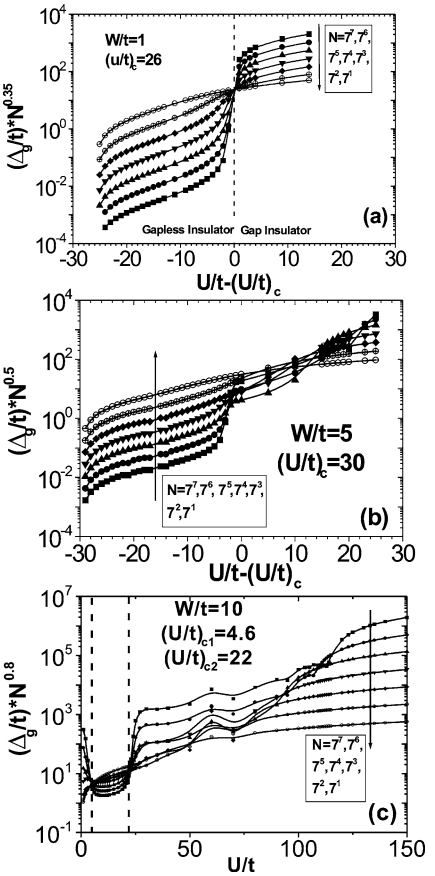

Fig. 4. Finite-size scaling analysis over the charge gap Δ_g/t against electron–electron interactions for fixed disorders. (a) $W/t = 1$. (b) $W/t = 5$. (c) $W/t = 10$.

identify the two phase transitions as discussed above, i.e., insulator–metal and metal–insulator transitions. But the last phase transition, Anderson insulator–Mott insulator is still absent in the finite-size scaling diagrams up to the magnitude of the disorders we have considered. It should be expected that one more critical point might appear if stronger disorders are considered. More extensive calculations are needed before a final conclusion can be drawn.

In summary, by using the BRG technique, we have investigated in detail the delicate interplay between disorders and electron–electron interactions on a half-filled triangular quantum dot lattice. The insulator–metal–insulator transition has been well demonstrated by the finite-size scaling analysis.

Acknowledgements

We would like to acknowledge the financial support of the Office of Naval Research (ONR).

References

[1] S.V. Kravchenko, G.V. Kravchenko, J.E. Furneaux, V.M. Pudalov, M. D'Iorio, Phys. Rev. B 50 (1994) 8039.
[2] E. Abrahams, S.V. Kravchenko, M.P. Sarachik, Rev. Mod. Phys. 73 (2001) 251, and references therein.
[3] S.J. Papadakis, E.P. de Poortere, H.C. Manoharan, M. Shayegan, E. Winkler, Science 283 (1999) 2056.
[4] Y. Yaish, O. Prus, E. Buchstab, S. Shapira, Y.G. Ben, U. Sivan, A. Stern, Phys. Rev. Lett. 84 (2000) 4954.
[5] B.L. Altshuler, D.L. Maslov, Phys. Rev. Lett. 82 (1999) 145.
[6] S.D. Sarma, E.H. Hwang, Phys. Rev. Lett. 83 (1999) 164.
[7] A.L. Dewalle, M. Pepper, C.J.B. Ford, E.H. Hwang, S.D. Sarma, D.J. Paul, G. Redmond, Phys. Rev. B 66 (2002) 075324.
[8] E. Abrahams, P.W. Anderson, D.C. Licciardello, T.V. Ramakrishnan, Phys. Rev. Lett. 42 (1979) 673.
[9] A.M. Finkelstein, Z. Phys. B: Condens. Matter 56 (1984) 189.
[10] C. Castellani, C. Di Castro, P.A. Lee, M. Ma, Phys. Rev. B 30 (1984) 527.
[11] Q. Si, C.M. Varma, Phys. Rev. Lett. 81 (1998) 4951; Q. Si, C.M. Varma, Physica B 259 (1999) 708.
[12] R. Kotlvar, S.D. Sarma, Phys. Rev. Lett. 86 (2001) 2388.
[13] F. Remacle, R.D. Levine, Chemphyschem. 2 (2001) 20; F. Remacle, R.D. Levine, Proc. Natl. Acad. Sci. 97 (2000) 553.
[14] P.J.H. Denteneer, R.T. Scalettar, N. Trivedi, Phys. Rev. Lett. 83 (1999) 4610.
[15] J.X. Wang, S. Kais, R.D. Levine, Int. J. Mol. Sci. 3 (2002) 4.
[16] F. Wegner, Z. Phys. B 36 (1980) 209.
[17] M. Imada, A. Fujimori, Y. Tokura, Rev. Mod. Phys. 70 (1998) 1039.
[18] T.W. Burkhardt, J.M.J. van Leeuwen (Eds.), Topics in Current Physics: Real-Space Renormalization, Springer-Verlag, Berlin, 1982.
[19] M. Ma, Phys. Rev. B 26 (1982) 5097.
[20] G. Caldara, B. Srinivasan, D.L. Shepelyansky, Phys. Rev. B 62 (2000) 10680.
[21] R. Berkovits, J.W. Kantelhardt, Y. Avishai, S. Havlin, A. Bunde, Phys. Rev. B 63 (2001) 085102.
[22] G. Benenti, X. Waintal, J. Pichard, Phys. Rev. Lett. 83 (1999) 1826.
[23] J.X. Wang, S. Kais, Phys. Rev. B 66 (2002) 081101(R).
[24] A. Andresen, C. Prasad, F. Ge, L.-H. Lin, N. Aoki, K. Nakao, J.P. Bird, D.K. Ferry, Y. Ochiai, Phys. Rev. B 60 (1999) 16050.
[25] A.R. Hamilton, M.Y. Simmons, M. Pepper, E.H. Linfield, P.D. Rose, D.A. Ritchie, Phys. Rev. Lett. 82 (1999) 1542.